

ARE DWARF GALAXIES DOMINATED BY DARK MATTER?

R. A. SWATERS¹

Department of Astronomy, University of Maryland, College Park, MD 20742

R. SANCISI

INAF - Osservatorio Astronomico di Bologna, via Ranzani 1, 40127 Bologna, Italy

and

Kapteyn Astronomical Institute, University of Groningen, Landleven 12, 9747 AD Groningen, the Netherlands

T. S. VAN ALBADA, J. M. VAN DER HULST

Kapteyn Astronomical Institute, University of Groningen, Landleven 12, 9747 AD Groningen, the Netherlands

ApJ, accepted

ABSTRACT

Mass models for a sample of 18 late-type dwarf and low surface brightness galaxies show that in almost all cases the contribution of the stellar disks to the rotation curves can be scaled to explain most of the observed rotation curves out to two or three disk scale lengths. The concept of a maximum disk, therefore, appears to work as well for these late-type dwarf galaxies as it does for spiral galaxies. Some of the mass-to-light ratios required in our maximum disk fits are high, however, up to about 15 in the *R*-band, with the highest values occurring in galaxies with the lowest surface brightnesses. Equally well-fitting mass models can be obtained with much lower mass-to-light ratios. Regardless of the actual contribution of the stellar disk, the fact that the maximum disk can explain the inner parts of the observed rotation curves highlights the similarity in shapes of the rotation curve of the stellar disk and the observed rotation curve. This similarity implies that the distribution of the total mass density is closely coupled to that of the luminous mass density in the inner parts of late-type dwarf galaxies.

Subject headings: Galaxies: dwarf – Galaxies: irregular – Galaxies: kinematics and dynamics

1. INTRODUCTION

Late-type dwarf galaxies are commonly thought to have slowly rising rotation curves and to be dominated by dark matter at all radii (e.g., Carignan & Beaulieu 1989; Persic et al. 1996; Côté et al. 2000). However, in a recent study of a large sample of late-type dwarf galaxies for which the rotation curves were derived in a uniform way, taking the effects of beam smearing into account, Swaters et al. (2009) found that the rotation curves of late-type dwarf galaxies have shapes similar to those of late-type spiral galaxies. For the dwarf galaxies in their sample, the rotation curves, when expressed in units of disk scale lengths, rise steeply in the inner parts and start to flatten at two disk scale lengths, as is usually seen in spiral galaxies (e.g., Broeils 1992a; Verheijen & Sancisi 2001). Such a difference in rotation curve shapes may have implications for the dark matter properties for late-type dwarf galaxies. We will investigate the implications for the Swaters et al. (2009) sample here.

For spiral galaxies, mass models based on the extended H I rotation curves indicate that large amounts of dark matter are required to explain the outer parts of observed rotation curves (e.g., van Albada et al. 1985; Begeman 1987; Broeils 1992a). In most of the galaxies in these studies, the inner parts of the observed H I rotation curves (out to two or three disk scale lengths) could be explained by scaling up the contribution of the stellar disk to the rotation curve, in agreement with findings based on optical rotation curves (Kalnajs

1983; Kent 1986). The same scaling, however, leaves large discrepancies in the outer parts of galaxies with H I rotation curves (van Albada & Sancisi 1986). This discrepancy is interpreted as evidence for the existence of large amounts of dark matter in galaxies. Alternatively, the observed discrepancy could be explained by a different theory of gravitation, such as MOND (Modified Newtonian Dynamics; Milgrom 1983; Sanders 1996).

The dark matter properties of galaxies are usually based on mass modeling of the rotation curves. If the contributions of the visible components are fixed, then whatever remains is the dark matter. A major obstacle is that the precise contribution of the stars to the rotation curve is not known, because the mass-to-light ratio of the stars is unknown. Upper limits to the mass-to-light ratios have been obtained by assuming that the contribution of the stellar disk is maximal (Kalnajs 1983; Kent 1986, 1987; Van Albada and Sancisi 1986). This ‘maximum disk’ solution minimizes the amount of dark matter required to explain the observed rotation curves. At the same time, as shown e.g., by van Albada & Sancisi (1986), the uncertainties in the stellar mass-to-light ratios allow for a range in mass models with different dark matter distributions.

Rotation curve studies of the dwarf galaxy DDO 154 (Carignan & Freeman 1988; Carignan & Beaulieu 1989) indicated, however, that this galaxy is dominated by dark matter at all radii, including the region well within the optical disk. Even when the contribution of the stellar disk is scaled as high as is allowed by the observed rotation curve (i.e., the maximum disk solution), the stellar disk could not be scaled to explain the observed rotation curves out to two or three disk scale lengths. The observations of DDO 154, along with stud-

rob@swaters.net

¹ Present address: National Optical Astronomy Observatory, 950 North Cherry Ave., Tucson, AZ 85719

ies of scaling relations based on relatively few well-studied dwarf galaxies (e.g., Casertano & van Gorkom 1991; Broeils 1992a; Persic et al. 1996), led to the generally accepted picture that dwarf galaxies have slowly rising rotation curves and are dominated by dark matter at all radii.

There are, however, also studies that provide a different picture, in which the stellar disks could be scaled to explain all of the inner rise of the rotation curves (e.g., Carignan 1985; Carignan et al. 1988; Lake et al. 1990; Broeils 1992b; Kim et al. 1998), suggesting that the dark matter properties may be similar to those of spiral galaxies.

A major problem is that in studies to date the galaxies have been observed with very different instrumental setups, and that the rotation curves were derived using different procedures, some of which may have been prone to introducing systematic errors (see e.g., Swaters et al. 2002; de Blok et al. 2008). Furthermore, the effects of beam smearing were not taken into account, even though these can be important (see e.g., Begeman 1987; Swaters et al. 2009).

In order to improve this situation we have obtained HI observations for a sample of 73 dwarf galaxies with a single instrument (Swaters 1999, hereafter S99; Swaters et al. 2002, hereafter Paper I), as well as *R*-band observations (Swaters & Balcells 2002, hereafter Paper II). From the HI observations, we derived rotation curves in a uniform way, taking into account the effects of beam smearing (S99; Swaters et al. 2009, hereafter Paper III). From this sample we have selected 18 high quality HI rotation curves for a detailed mass model analysis which we report in this paper.

The layout of this paper is as follows. In the next section we will describe the sample and the rotation curves. In Section 3 the different components that are used in the mass models and the fitting of these mass models to the rotation curves are described. Section 4 presents the results of the mass modeling. In Section 5 the results are discussed, and we present our conclusions in Section 6.

2. THE SAMPLE AND THE ROTATION CURVES

The late-type dwarf galaxies in this sample have been observed as part of the WHISP project (Westerbork HI Survey of Spiral and Irregular Galaxies; for a more detailed description of the WHISP project and its goals, see Paper I). The galaxies in the WHISP sample have been selected from the UGC catalog (Nilson 1973), taking all galaxies with declinations north of 20° , blue major axis diameters larger than $1.5'$ and measured flux densities larger than 100 mJy. From this list we selected the late-type dwarf galaxies, defined as galaxies with Hubble types later than Sd, supplemented with spiral galaxies of earlier Hubble types but with absolute *B*-band magnitudes fainter than -17 . For a detailed description of the selection criteria, see Paper I. Optical *R*-band data for all these galaxies are presented in Paper II, which also includes a discussion of the distance uncertainties for the galaxies presented here.

The sample of late-type dwarf galaxies used here is selected from the sample of 62 late-type dwarf galaxies for which rotation curves could be derived in Paper III. Here, we only selected galaxies with high quality rotation curves (classified as such in Paper I) and with inclinations in the range $39^\circ \leq i < 80^\circ$ (but mass models for galaxies with lower-quality rotation curves galaxies were presented by S99). The lower limit of 39° was chosen to also include UGC 12732. Note that edge-on galaxies have been excluded, because their rotation curves are difficult to determine, and also because the radial distributions of the gas and especially that of the light

from the stellar disk are difficult to measure. We excluded UGC 11861 because of its high luminosity. The resulting sample, listed in Table 1, contains 18 galaxies.

It is possible that some of the galaxies in our sample are affected by noncircular motions. However, because the galaxies were selected from the larger sample presented in Paper III to be symmetric in nature, it is unlikely noncircular motions play an important role. Moreover, because the rotation curves have been derived by averaging over annuli, effects from noncircular motions are minimized.

As can be seen in Table 1, most of the galaxies in our sample have absolute magnitudes fainter than $M_R = -18$, as expected for dwarf galaxies. Some are a little brighter than $M_R = -18$, because the initial sample selection, described in detail in Paper I, was in part based on morphological type, and because of uncertainties in the determination of the absolute magnitudes that were used in the initial sample selection.

Most of the late-type dwarf galaxies have small exponential disk scale lengths. The median value for the scale length is 1.6 kpc, and 5 galaxies have scale lengths of less than 1 kpc. However, 7 galaxies have scale lengths larger than 2 kpc, and 5 of these have surface brightnesses lower than $\mu_R = 22$ mag. These galaxies have properties that are similar to those of the class of low surface brightness (LSB) galaxies studied by e.g., de Blok et al. (1995).

The rotation curves have been derived with an interactive procedure, as described in detail in Paper III. First an estimate of each rotation curve was made based on a simultaneous fit by eye to six position-velocity diagrams with different position angles. Next, each rotation curve was refined by constructing a model data cube, based on the input rotation curve, and then adjusting the rotation curve to find the best match between the model cube and the observed data cube. As the comparison with high-resolution $H\alpha$ data in Paper III showed, this procedure made it possible to correct for the effects of beam smearing to a large degree.

3. MASS MODELS

The circular velocity is a direct reflection of the gravitational potential of a galaxy, assuming it is axially symmetric and in equilibrium:

$$F_r = \frac{\partial\Phi}{\partial r} = -\frac{v_c^2}{r}, \quad (1)$$

where F_r is the radial force, Φ the gravitational potential, r the radius and v_c the circular velocity. As was discussed in Paper III, the corrections for asymmetric drift tend to be uncertain because the gas pressure usually cannot be determined accurately. Because the corrections are expected to be small (less than 1 km s^{-1} in the inner parts of the rotation curves and less than 3 km s^{-1} at all radii for 95% of the galaxies presented here), the observed rotation curves were used to represent the circular velocities.

The gravitational potential is the sum of the gravitational potentials of the individual mass components in each galaxy. Expressed in velocities, this sum becomes

$$v_{\text{rot}}^2 = v_*^2 + v_g^2 + v_h^2, \quad (2)$$

with v_* the contribution of the stellar disk to the rotation curve, v_g the contribution of the gas and v_h that of the dark halo. In Equation 2 the contribution of a bulge component is left out because the galaxies in this sample have little or no bulge. Since we have no prior knowledge of the stellar

TABLE 1
 OPTICAL AND DARK MATTER PROPERTIES

UGC (1)	D_a (2)	M_R (3)	h (4)	μ_{00}^R (5)	$S_{(2,3)}^h$ (6)	i (7)	maximum disk				minimum disk			$\Upsilon_*^R = 1$		
							Υ_*^R (8)	ρ_0 (9)	r_c (10)	χ_r^2 (11)	ρ_0 (12)	r_c (13)	χ_r^2 (14)	ρ_0 (15)	r_c (16)	χ_r^2 (17)
731	8.0	-16.6	1.65	23.0	0.34	57	15.1	1.6±0.3	∞	0.45	170±30	0.8±0.1	0.23	150±30	0.81±0.09	0.22
3371*	12.8	-17.7	3.09	23.3	0.18	49	12.5	1.1±0.2	∞	0.73	37±6	2.1±0.2	0.85	32±6	2.2±0.3	0.82
4325	10.1	-18.1	1.63	21.6	0.08	41	9.1	—	—	1.81	330±80	0.8±0.1	1.77	300±70	0.75±0.10	1.49
4499	13.0	-17.8	1.49	21.5	0.30	50	2.3	14±5	2.8±0.7	0.58	65±15	1.3±0.2	0.15	37±10	1.7±0.3	0.22
5414	10.0	-17.6	1.49	21.8	—	55	4.6	—	—	1.13	44±12	1.5±0.3	0.14	30±8	1.7±0.4	0.18
6446	12.0	-18.4	1.87	21.4	0.17	52	4.0	5.3±1.5	6.2±1.6	0.39	200±40	0.8±0.1	0.16	120±20	0.95±0.10	0.05
7323	8.1	-18.9	2.20	21.2	—	47	3.0	2.6±0.8	∞	0.39	50±12	2.0±0.3	0.66	27±8	2.7±0.7	0.30
7399	8.4	-17.1	0.79	20.7	0.27	55	7.7	31±4	3.0±0.3	1.27	510±80	0.6±0.1	0.98	370±60	0.76±0.08	0.97
7524*	3.5	-18.1	2.58	22.2	0.24	46	7.2	1.4±0.3	∞	0.27	73±8	1.4±0.1	0.44	59±7	1.5±0.1	0.29
7559	3.2	-13.7	0.67	23.8	0.15	61	13.1	6.1±2.0	∞	0.22	100±40	0.5±0.2	0.09	90±40	0.55±0.21	0.09
7577	3.5	-15.6	0.84	22.5	—	63	0.9	—	—	0.40	8±4	0.8±0.3	0.15	0	—	0.63
7603	6.8	-16.9	0.90	20.8	0.54	78	4.1	7.9±2.5	4.9±1.8	0.84	100±20	0.9±0.1	0.30	64±18	1.2±0.2	0.17
8490	4.9	-17.3	0.66	20.5	0.29	50	4.4	35±10	1.9±0.3	0.39	1100±200	0.33±0.04	0.34	570±150	0.44±0.05	0.20
9211	12.6	-16.2	1.32	22.6	0.41	44	11.2	5.2±2.2	5.1±2.1	0.58	86±26	1.0±0.2	0.31	72±24	1.1±0.2	0.24
11707*	15.9	-18.6	4.30	23.1	0.14	68	9.3	0.7±0.1	∞	0.83	61±21	1.7±0.3	0.42	49±16	1.8±0.4	0.42
12060	15.7	-17.9	1.76	21.6	0.07	40	8.3	0.5±0.2	∞	0.18	500±200	0.45±0.14	0.55	400±160	0.48±0.15	0.36
12632*	6.9	-17.1	2.57	23.5	0.16	46	15.1	1.0±0.2	∞	1.06	110±20	1.0±0.2	0.12	100±20	1.0±0.2	0.13
12732*	13.2	-18.0	2.21	22.4	0.27	39	7.5	2.0±0.4	16±7	0.37	74±18	1.4±0.2	0.17	53±16	1.6±0.3	0.24

NOTE. — (1) UGC number; galaxies labeled with a * have properties similar to LSB galaxies (2) adopted distance in Mpc, from Paper II, (3) absolute R -band magnitude from Paper II, (4) R -band scale length in kpc from Paper II, (5) extrapolated central R -band disk surface brightness, from Paper II, (6) logarithmic rotation curve shape between 2 and 3 disk scale lengths, from Paper III, (8) inclination, from Paper III, (9) maximum disk mass-to-light ratio, in units of M/L_\odot , (10,12,14) central halo density, in units of $10^{-3} M_\odot \text{pc}^{-3}$, (11,13,15) core radius in kpc.

mass-to-light ratio, some value Υ_* has to be assumed. The contribution of the gas to the rotation curve includes the contribution of helium. This scaling of the H I is represented by η . Making this explicit, Equation 2 becomes

$$v_{\text{rot}} = \sqrt{\Upsilon_* v_d^2 + \eta v_{\text{HI}}^2 + v_h^2}, \quad (3)$$

where v_d is the contribution of the stellar disk for a stellar mass-to-light ratio of unity, and v_{HI} is that of the H I only. Each of the individual components in this equation is described below.

3.1. The contribution of the stellar disk

The R -band luminosity profiles presented in Paper II have been used to calculate the contribution of the stellar disk to the observed rotation curve, assuming the mass-to-light ratio Υ_*^R is independent of radius. Because most of the galaxies in this sample have light profiles that are well represented by an exponential disk, and generally have little or no bulge, the light profiles were not decomposed into a disk and a bulge component. The contribution of the stellar disk to the rotation curve was calculated using the prescription given in Casertano (1983), assuming that the galaxies are optically thin and assuming an intrinsic thickness of $q_0 = 0.2$. This value was chosen because it appears to be a suitable value for the average of the intrinsic thickness over the range of galaxy types included in this sample. Late-type disk galaxies, of morphological types around Sd, are reported to have intrinsic thicknesses closer to $q_0 = 0.1$ (e.g., de Grijs 1997; Schwarzkopf & Dettmar 2000; Bizyaev & Kajsın 2004), but for late-type dwarf galaxies higher values may be found, up to $q_0 = 0.4$, especially towards the lowest luminosity systems (van den Bergh 1988; Binggeli & Popescu 1995; Sung et al. 1998). We estimate the uncertainty in the amplitude of the rotation curve introduced by the variations in q_0 from galaxy to galaxy to be $\sim 5\%$ (see S99 for more details).

The major uncertainty in determining a mass model for a galaxy is the mass to light ratio Υ_* , which is not known a priori and cannot be derived from the rotation curve fits alone. Equally well fitting mass models can be obtained with a range in Υ_* (e.g. van Albada et al. 1985; Swaters et al. 2000, 2003; Dutton et al. 2005; see also Section 4). However, it is possible to obtain limits on Υ_* by scaling up the contribution of the stellar disk to explain most of the observed rotation curve in the inner parts (the so-called maximum disk hypothesis), and by reducing the contribution of the stellar disk to its minimum while still obtaining a good fit to the rotation curve.

3.2. The contribution of the gas

The procedure for deriving the contribution of the gas to the rotation curve is very similar to that of the stellar disk. The H I radial profiles presented in Paper I were used to calculate this contribution. We assumed that the gas layer has an intrinsic thickness of $q_0 = 0.2$, the same value that was assumed for the thickness of the stellar disk. Little is known about the vertical distribution of the gas in late-type dwarf galaxies. There is some evidence that the gas and the stars have the same vertical distribution (Bottema et al. 1986). Fortunately the precise choice of the thickness of the H I layer has very little influence on the shape or amplitude of the rotation curve and the uncertainty is smaller than that introduced by assuming a constant thickness of $q_0 = 0.2$ for the optical disk.

In order to derive the contribution of the gas to the rotation curve, the H I was assumed to be optically thin. To correct for the mass fraction of helium, the H I mass was scaled by a factor $\eta = 1.32$, derived assuming a primordial Helium fraction of 24% (Steigman 2007).

Other gas components that might contribute to the rotation curve, such as molecular hydrogen, have been ignored. To date, most evidence suggests there is much less molecular hydrogen in late-type dwarf galaxies than there is H I, even when taking into account that the conversion factor to convert the

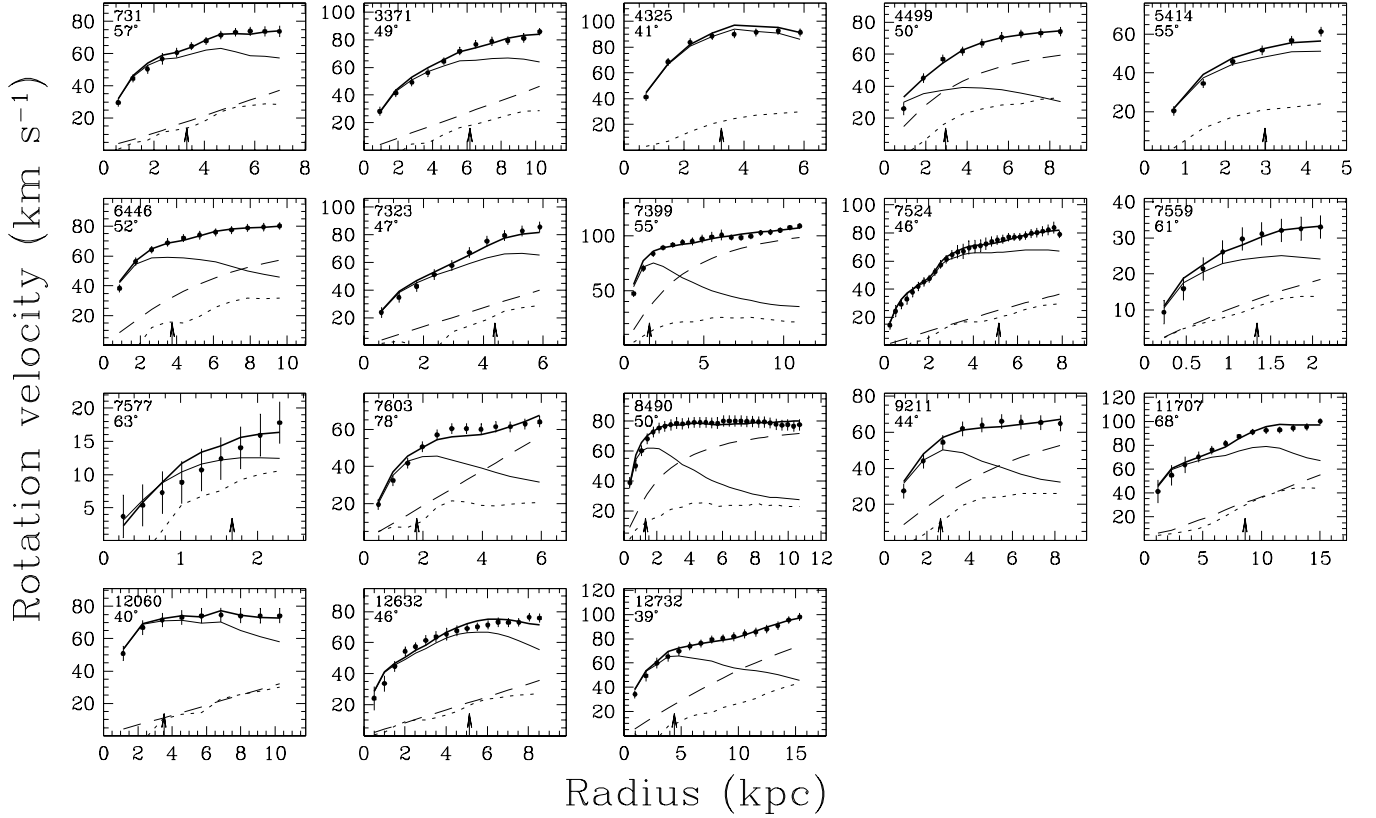


FIG. 1.— Maximum disk mass models. The filled circles represent the derived rotation curves. The thin full lines represent the contribution of the stellar disks to the rotation curves, the dotted lines that of the gas and the dashed lines that of the dark halos. The thick solid lines represent the maximum disk mass models. The arrows at the bottom of each panel indicate a radius of two disk scale lengths. In the top left corner of each panel the UGC number and the inclination are given.

observed CO flux into a molecular gas column density may be substantially higher in late-type dwarf galaxies (e.g., Israel et al. 1995; Boselli et al. 2002; Buyle et al. 2006). Moreover, if molecular gas were to have the same radial distribution as the stellar disk, its contribution is implicitly included in the maximum disk fits.

3.3. The contribution of the dark halo

Several different halo radial mass profiles have been proposed over the years, most of which produce good fits to the observed rotation curves. Halo mass-density profiles as predicted by cosmological simulations have received a great deal of attention, because a confrontation of these profiles against the observed rotation curves provides a powerful test of these cosmological models. For most of the sample presented here, such tests have been presented in van den Bosch & Swaters (2001) and Swaters et al. (2003).

In this paper, we focus on an empirical description of the properties of the dark matter halos. For this purpose, we have used the density profile of an isothermal sphere that has often been used in the literature to represent the dark halo. The advantage is that it will be easier to compare our results with those of other studies (e.g., Broeils 1992a; Verheijen 1997; Noordermeer 2006; see also Section 5.2).

The radial density profile of an isothermal sphere can be approximated by

$$\rho(r) = \rho_0 \left[1 + \left(\frac{r}{r_c} \right)^2 \right]^{-1}, \quad (4)$$

where ρ_0 is the central density of the halo, and r_c the core radius. This density profile gives rise to a rotation curve of the following form

$$v_h(r) = \sqrt{4\pi G \rho_0 r_c^2 \left[1 - \frac{r_c}{r} \arctan \left(\frac{r}{r_c} \right) \right]}. \quad (5)$$

3.4. Rotation curve fits

The relative contribution of each of the three components described above is determined by a simultaneous fit of the right-hand side of Equation 3 to the observed rotation curve. For an isothermal halo, there are four free parameters in Equation 3. However, the contribution of the atomic gas to the rotation curve is known, and therefore, with the correction for the mass fraction of helium, η is fixed to 1.32. On the other hand, the value of Υ_* is not known beforehand, and a range of Υ_* and halo parameters exists which produce a good fit to the data (van Albada et al. 1985). Mathematically, it is possible to derive the parameters for the isothermal halo and the value of Υ_* from a best fit to the observed rotation curve. However, the physical meaning of such a best fit is unclear, as the values found from such a fit depend on the small scale variations and uncertainties in the rotation curves. Because of these uncertainties in Υ_* , two limiting cases are presented. In one case, the contribution of the stellar disk is scaled up to explain most of the rotation curve out to two or three disk scale lengths. This is the maximum disk solution. In the other limiting case, the contribution of the stellar disk is completely ignored, and the rotation curve is fitted with the contributions of dark halo

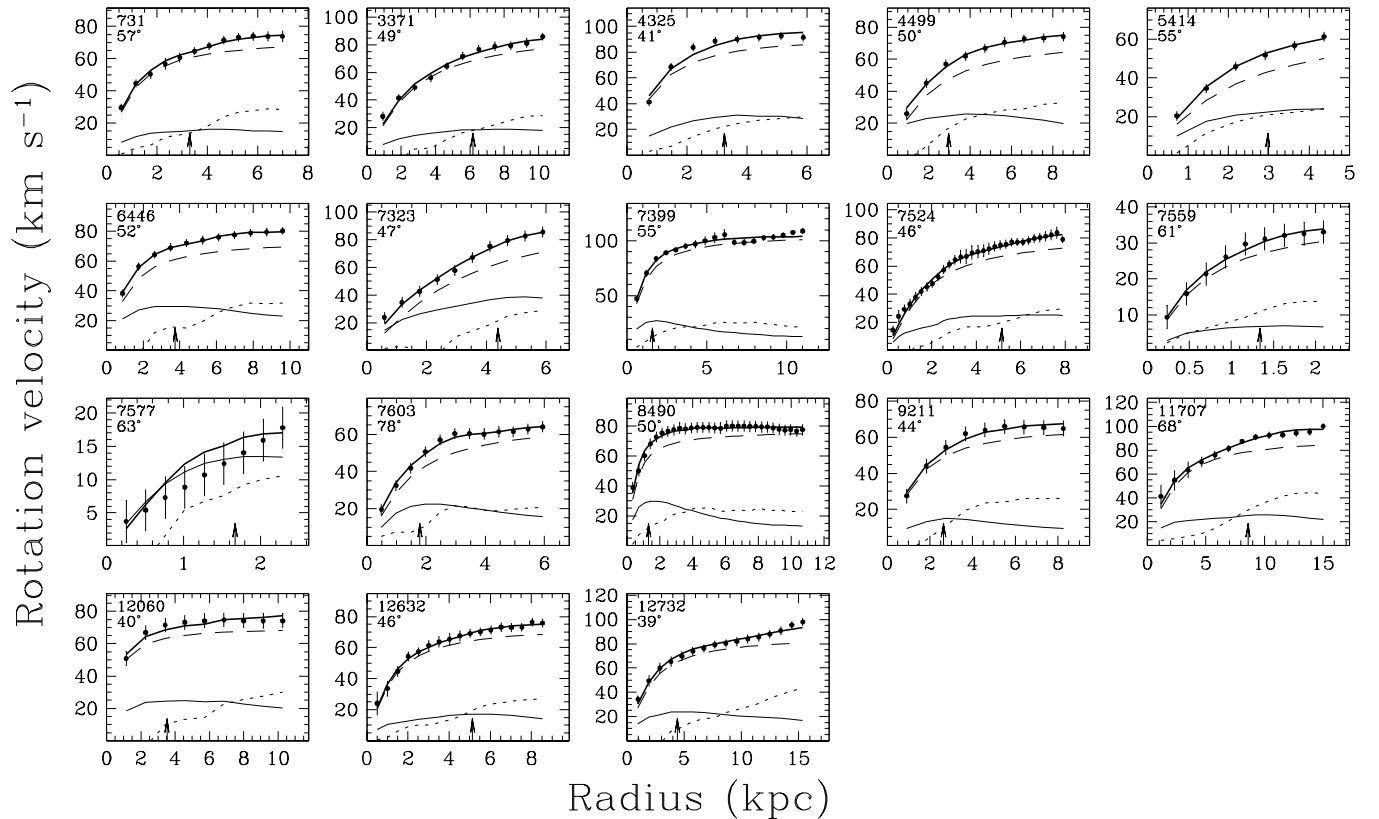


FIG. 2.— Same as Figure 1, but for the $\Upsilon_*^R = 1$ models.

and gas only.

The maximum disk fits were done by eye, ensuring that the rotation curve of the stellar disk contributes maximally to the observed rotation curve within its observational uncertainties, following e.g., Broeils (1992a), Verheijen (1997), and Noordermeer (2006). We have refit several mass models from the literature using our methods. We were able to reproduce the original results to better than 10 percent. A mass model is only considered to be compatible with a maximum disk if the stellar disk can be scaled up to explain at least $\sim 80\%$ of the rotation velocity at 2.2 disk scale lengths (e.g., Sackett 1997; see also Section 5.1).

There has been considerable effort over the past decade to relate the broad-band colors of galaxies to their Υ_* through stellar population synthesis modeling (e.g., Bell & de Jong 2001; Bell et al. 2003; Zibetti et al. 2009). The advantage of using such models is that it provides an independent estimate of Υ_* and possibly a more realistic value of Υ_* . However, there is some uncertainty in Υ_* as derived from population synthesis modeling, because of, for example, uncertainties in the star formation history, the initial stellar mass function, metallicity, and the details of the late-phases of stellar evolution. The combined uncertainty may be a factor 4 or even larger if some of uncertainties are systematic (see e.g., Ber-shady et al. 2010).

The six galaxies in our sample with both B and R -band observations presented in Paper II have an average $B-R$ color of 0.8 mag. Following Bell et al. (2003), this corresponds in $\Upsilon_*^R \sim 0.8$, although this value of Υ_*^R is uncertain, as discussed above. However, for any Υ_*^R near unity, all but one of the galaxies in our sample are completely dominated by dark matter, so the exact choice of Υ_*^R has little influence on

the derived dark halo parameters (see also Section 4). Given these considerations, and because we had already calculated the contribution of the stellar disk for $\Upsilon_*^R = 1$ for the input of the mass modeling, we used these to determine the dark halo properties in these population synthesis-based restricted- Υ_* fits.

The rotation curve fits are shown in Figures 1 and 2. The minimum disk fits are not shown separately because in most cases the mass models are very similar to those for $\Upsilon_*^R = 1$. The fit parameters are given in Table 1. The uncertainties on the fitted parameters have been derived from the 68% confidence levels and include the covariance between ρ_0 and r_c . The uncertainties on the derived rotation velocities are non-Gaussian, as the points in the rotation curves are correlated, and the rotation curves and their uncertainties can be affected by systematic effects. The confidence levels and the corresponding uncertainties should be considered estimates.

4. RESULTS FROM FITTING MASS MODELS

In this section we will present the results from fitting the different mass models: maximum disk, minimum disk, and fixed Υ_*^R .

4.1. Maximum disk fits

The most striking result from the maximum disk fits, presented in Figure 1, is that in all 18 galaxies the contribution of the stellar disk can be scaled up to explain most of the inner parts of the rotation curves out to two or three disk scale lengths, with the exception of UGC 4499. Thus, it seems that the fact that the stellar disk can be scaled to explain most of the inner parts of the rotation curves of late-type dwarf galaxies is rule rather than exception. This is in contrast with the re-

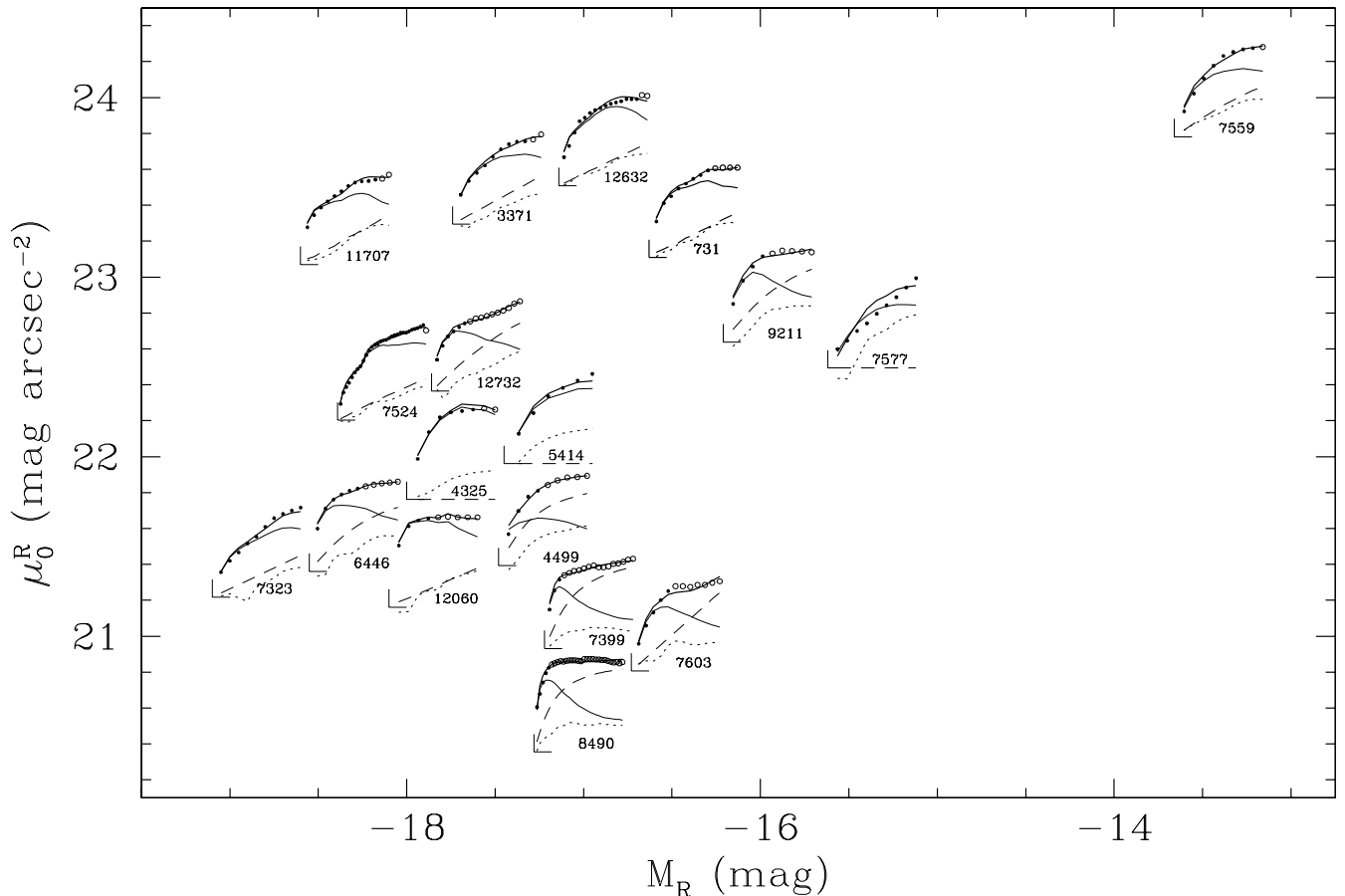


FIG. 3.— Rotation curves and the fitted maximum disk mass models plotted as a function of absolute magnitude M_R and central disk surface brightness μ_0^R . The origin of each rotation curve indicates the corresponding M_R and μ_0^R of that galaxy. Where necessary, the rotation curves have been shifted slightly to avoid overlap between the different rotation curves. The rotation curve data are represented by circles, filled circles for radii smaller than three disk scale lengths, open circles for large radii. Coding of the lines is the same as in Figure 1. The rotation curves have been scaled by maximum velocity and radius of the last measured point. Note that the relative contribution of the stellar disk to the rotation curve does not appear to depend on absolute magnitude or surface brightness.

sults from several previous studies of dwarf galaxies, in which the stellar disk only can explain a small fraction of the inner rise; this is examined in more detail in Section 5.2.

To illustrate how the maximum disk mass models depend on the optical galaxy properties, we have plotted the mass models against surface brightness and absolute magnitude in Figure 3. In this figure, the origin of each model indicates the μ_R and M_R for each galaxy. The rotation curves are represented by filled circles for radii smaller than three disk scale lengths, and by open circles for larger radii. From an inspection of Figure 3 it appears that there is no clear trend between the relative contribution of the stellar disk to the rotation curve on the one hand, and rotation curve shape, luminosity or surface brightness on the other. Maximum disks are seen at all surface brightnesses and all absolute magnitudes.

This point is demonstrated in more detail in Figures 4 and 5. Figure 4 shows that there is no clear correlation between the rotation curve shape as determined by the logarithmic slope between two and three disk scale lengths $S_{(2,3)}^h$, and the relative contribution of the stellar disk to the rotation curve at 2.2 disk scale lengths (see Paper III for details). Independent of the rotation curve shape, the contribution of the stellar disk to the rotation curve is about 90% at 2.2 disk scale lengths. Figure 4 also shows the correlation between rotation curve shape and the relative contribution of the stellar disk at four disk scale lengths. The contribution of the stellar disk to the ro-

tation curve has dropped to about 70%. There is one galaxy, UGC 12060, where even at four disk scale lengths the stellar disk can still explain most of the observed rotation curve. This galaxy has excess light between three and four disk scale lengths, when compared to an exponential fall-off.

From Figure 5 it is clear that the maximum disk hypothesis works equally well for all surface brightnesses.

From the results presented here, it is apparent that for the vast majority of these late-type dwarf galaxies the contributions of their stellar disks to the rotation curves can be scaled to explain most of the inner parts of the observed rotation curves. Therefore, these dwarf galaxies do not necessarily have insignificant mass in their stellar disks and dominant dark halos, as concluded in earlier work. For the maximum disk fits, dark matter only becomes important at radii larger than three or four disk scale lengths. These maximum disk mass models for late-type dwarf galaxies are similar to those seen in spiral galaxies (e.g., Begeman 1987; Broeils 1992a; Verheijen 1997).

4.1.1. Stellar mass-to-light ratios

Although for the majority of the late-type dwarf galaxies in our sample the contribution of the stellar disk can explain most of the rotation curve in the inner parts, the stellar mass-to-light ratios Υ_*^R may be high. In Figure 6 a histogram is presented of the derived values of Υ_*^R for the maximum disk

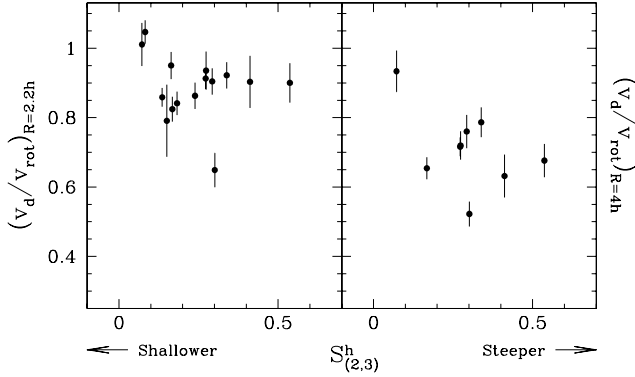


FIG. 4.— Relative contribution of the stellar disk to the rotation curve for the maximum disk fits at 2.2 disk scale lengths (left panel) and at 4 disk scale lengths (right panel) versus logarithmic slope between two and three disk scale lengths $S_{(2,3)}^h$.

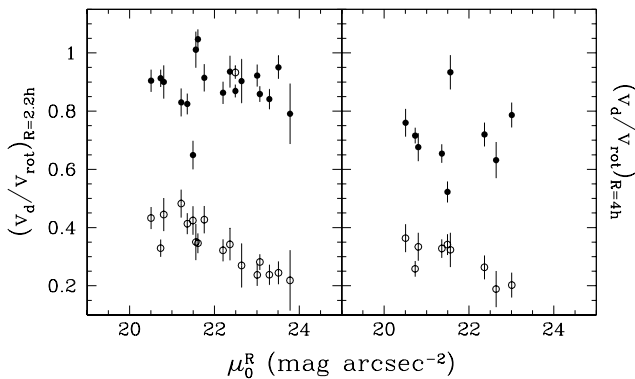


FIG. 5.— Relative contribution of the stellar disk to the rotation curve for the maximum disk fits (filled circles) and fits with $\Upsilon_*^R = 1$ (open circles) at 2.2 disk scale lengths (left panel) and at 4 disk scale lengths (right panel) versus central disk surface brightness μ_0^R .

fits. The average value for Υ_*^R is 7.7, but ranges from 1 to 15, with the high end being well outside the range predicted by current population synthesis models. These high values of Υ_*^R will be discussed in more detail in Section 5.

Figure 7 shows Υ_*^R plotted against the central surface brightness μ_R and the absolute magnitude M_R . Galaxies with lower surface brightnesses have higher values for Υ_*^R under the assumption of maximum disk (see also section 5.3).

4.1.2. Isothermal halo properties

In three cases (UGC 4325, UGC 5414 and UGC 7577), the rotation curve can be explained by the stellar disk and the H I alone; see Figure 1. Hence, the fitted dark halos will have central densities close to zero, and the core radii are not constrained. For several galaxies with more extended rotation curves (see Figure 2), the rotation curves of the dark halos have a solid body appearance, indicating that the dark matter halos have constant density cores. In these cases, the core radius is also unconstrained and only the halo density can be determined. Only for eight galaxies with sufficiently extended rotation curves both the core radius and the central density can be determined reliably.

Figure 8 shows that the core radius r_c and the disk scale length h are correlated. The halo core radius is on average 3.5 ± 0.5 times as large as the disk scale length. A similar ratio of 3.0 ± 0.5 is found for the spiral galaxies presented

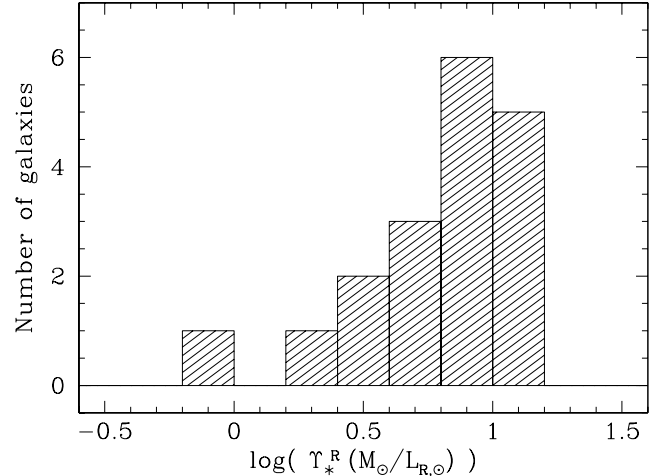


FIG. 6.— Distribution of maximum disk R -band mass to light ratios Υ_*^R .

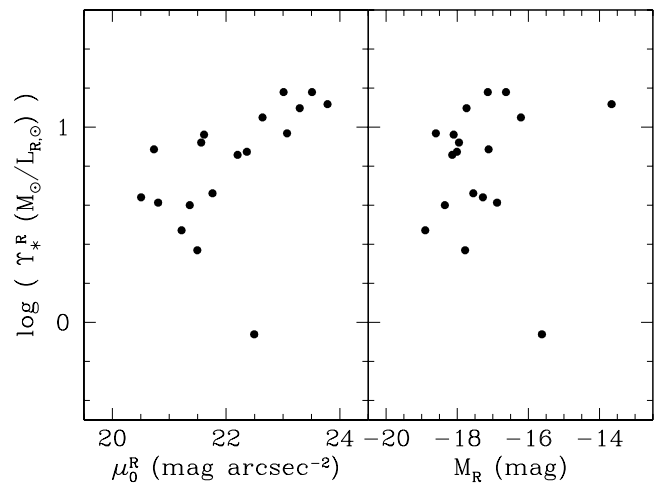


FIG. 7.— R -band stellar mass-to-light ratios Υ_*^R as determined from the maximum disk fits versus central disk surface brightness μ_0^R (left panel) and versus absolute R -band magnitude M_R (right panel).

in Broeils (1992a), demonstrating the similarity between the maximum disk fits of the late-type dwarf galaxies in our sample and those of spiral galaxies. Such a ratio of core radius to disk scale length of about three is expected for galaxies with a more or less flat rotation curve, as was also mentioned by van Albada & Sancisi (1986), who found that the expected ratio is about 3.5.

For scaling relations between the optical properties of the galaxies in our sample and the relative fractions of mass in stars, gas, and dark matter, we refer to S99.

Note from Figure 1 that in the case of maximum disk models the shapes of the halo rotation curves often are similar to the shapes of the gas rotation curves. This is remarkable and indicates that the ratio of dark matter surface density to gas surface density is constant in the outer parts. This was noted for spiral galaxies by Bosma (1981) and further investigated by Hoekstra et al. (2001). A detailed study of the apparent link between the H I and dark matter densities will be the subject of an upcoming paper.

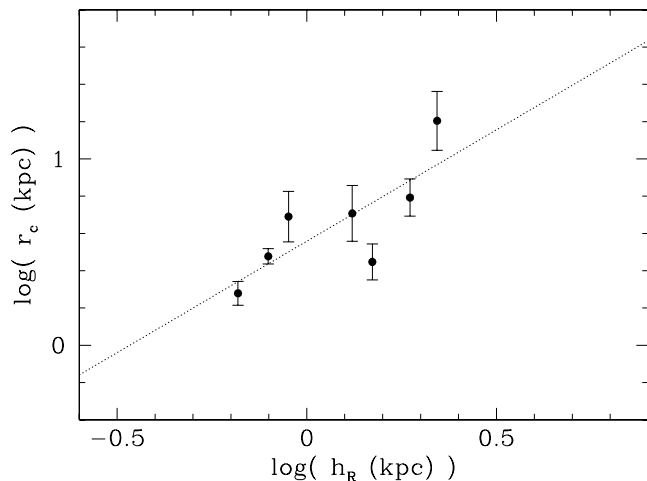


FIG. 8.— Halo core radius versus R -band optical disk scale length for the maximum disk fits, for those galaxies for which the core radius could be reliably determined.

4.2. Fits with fixed mass-to-light ratios

A lower limit to the contribution of the stellar disk to the rotation curve can be obtained by decreasing Υ_*^R to its lowest possible value while the mass model still produces a good fit to the rotation curve. For the late-type dwarf galaxies in this sample, the rotation curves can be well fitted using only a dark halo and the H I (i.e., $\Upsilon_*^R = 0$). A minimum disk fit thus does not provide a useful lower limit on Υ_*^R , but it does provide an upper limit on the halo mass within a given radius and on the central density, and a lower limit on the halo core radius. The results for the minimum disk fits are given in Table 1. The mass models themselves are not shown because the dark halos are very similar to those for $\Upsilon_*^R = 1$, shown in Figure 2. Details of the correlations between the minimum-disk dark halo properties and optical properties were presented in S99.

As was shown above, and as will be discussed in more detail in Section 5, the maximum-disk Υ_*^R values are higher than expected from population synthesis models. To investigate the dark halo properties for values of Υ_*^R that are in agreement with population synthesis models (as was described in Section 3.4), we also fit mass models for $\Upsilon_*^R = 1$. The results of the fits are presented in Table 1, and the fits themselves are shown in Figure 2.

With $\Upsilon_*^R = 1$, the relative contribution of the stellar disk to the rotation curve is tightly correlated with surface brightness, as can be seen in Figure 5. Such a tight correlation is expected for models with a fixed Υ_*^R , because in that case the surface brightness is directly linked to the surface mass density and hence to the relative contribution of the stellar disk.

5. DISCUSSION

5.1. Main result

The main result of the present study is that the contribution of the stellar disk can be scaled up (“maximum disk”) to explain the inner parts of the rotation curve of all but one of the 18 late-type galaxies in the present sample. These maximum disk models are similar to those for late-type spiral galaxies in which the stellar disks can also be scaled to explain the inner rotation curves (e.g., Kalnajs 1983; Kent 1987; Begeman 1987; Broeils 1992a; Verheijen 1997) and also those of the LSB galaxies presented in Swaters et al. (2000; 2003).

How well maximum disk works is described by ξ the frac-

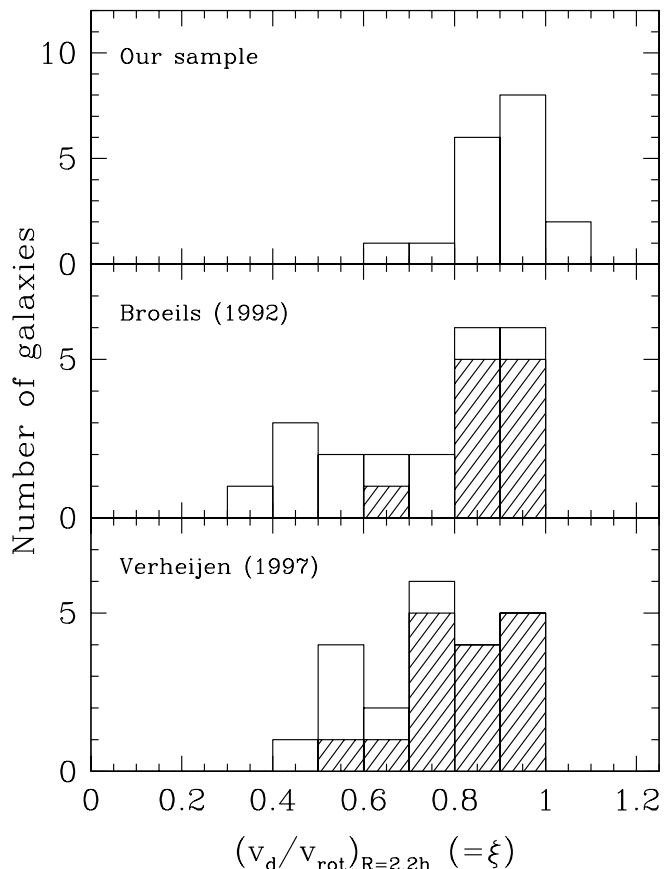


FIG. 9.— Distribution of the fractional contribution of the maximum stellar disk to the rotation curve at 2.2 disk scale lengths for the galaxies in our sample, and the samples presented in Broeils (1992a) and Verheijen (1997). The shaded areas represent galaxies with numeric Hubble types earlier than Sd, the open areas represent galaxies with Hubble type Sd or later.

tional contribution of the maximum stellar disk to the rotation curve at two disk scale lengths. A low value for ξ means that even when scaled as high as possible, the stellar disk can only explain a small fraction of the observed rotation curve. A high value of ξ (near unity) means that the stellar disk can be scaled to explain most or all of the observed rotation curve.

For the galaxies in our sample $\xi = 0.88$, with a dispersion around the mean of 0.09. This is nearly identical to the average for the spiral galaxies in the sample of Broeils (1992a), for which $\xi = 0.86 \pm 0.07$, and to the average for spiral galaxies in the Verheijen (1997) sample, with $\xi = 0.81 \pm 0.12$ (see Figure 9).

If we assume that the values for ξ near unity mean that these dwarf galaxies physically have maximal disks (despite the high required mass-to-light ratios), then the stellar disk can explain the mass distribution over the optical parts of the galaxy, and dark matter only becomes relevant at large radii.

Under the same assumption, the average ratio of stellar-to-dark mass within four disk scale lengths is 1.0 ± 0.6 for the dwarf galaxies in our sample. For the spiral galaxies in the sample presented in Broeils (1992a) the average stellar-to-dark mass ratio within four disk scale lengths is 0.9 ± 0.4 . Thus, the maximum disk fits for dwarf galaxies and spiral galaxies are very similar, with similar relative amounts of mass in the dark and luminous components within similar numbers of disk scale lengths. In these maximum disk fits, dwarf galaxies are not dominated by dark matter at all radii. Dark matter is only needed to explain the outer part of the

rotation curve.

5.2. Comparison with previous work

The conclusion reached here contrasts with the general notion from previous work that in late-type dwarf galaxies dark matter dominated everywhere. The average value of ξ in the comparison samples of Broeils (1992a) and Verheijen (1997) when including only late-type dwarf galaxies is lower than what we find here. For the late-type dwarf galaxies in the sample of Broeils (1992a), $\xi = 0.61 \pm 0.20$, and for the Verheijen (1997) sample, $\xi = 0.58 \pm 0.09$. Such lower values of ξ are found when a rotation curve rises slowly.

Indeed, the conclusion that the stellar disk cannot be scaled to explain the inner rise of the observed rotation curve is reached in many of the dark matter studies of late-type dwarf galaxies, e.g. DDO 154 (Carignan & Freeman 1988, Carignan & Beaulieu 1989), NGC 300 (Puche et al. 1990), NGC 55 (Puche et al. 1991), NGC 3109 (Jobin & Carignan 1990), NGC 5585 (Côté et al. 1991), DDO 168 (Broeils 1992a), IC 2574 (Martimbeau et al.), NGC 2915 (Meurer et al. 1996), five dwarfs in the Sculptor and Centaurus A groups (Côté et al. 1997; see also Côté 1995), NGC 5204 (Sicotte & Carignan 1997), NGC 2976 (Simon et al. 2003), and NGC 6822 (Weldrake et al. 2003). Many of these studies have led to the notion that dwarf galaxies are dominated by dark matter at all radii.

There are, however, also studies that provide a different picture. Some early mass models for late-dwarf galaxies showed that the stellar disk could be scaled to explain all of the inner rise of the rotation curves, suggesting that the dark matter properties of these galaxies were similar to those of spiral galaxies (Carignan 1985; Carignan, et al. 1988). Similar results were found for the four late-type dwarf galaxies in the Virgo clusters studied by Skillman et al. (1987), DDO 170 (Lake et al. 1990), DDO 105 (Broeils 1992a), NGC 1560 (Broeils 1992b), most of the late-type dwarf galaxies presented in van Zee et al. (1997), the Large Magellanic Cloud (Kim et al. 1998; Bekki & Stanimirovic 2009), and most of the galaxies presented in S99 and Swaters et al. (2003).

The spread in results seen in earlier studies raises the question whether the spread reflects an intrinsic spread in the rotation curve shapes of dwarf galaxies, which then results in a range of different mass models, or whether this observed spread is due to other factors that affect the derived rotation curves.

There are well-known systematic effects that can affect the shape of the derived rotation curve and can make it appear shallower. For example: (i) beam smearing can wash out steep gradients and make the inner rotation curve appear more shallow (e.g., Begeman 1987; Paper III); (ii) rotation curves derived from high-inclination galaxies are susceptible to underestimated velocities in the inner parts (e.g., Sancisi & Allen 1979; Swaters et al. 2003); (iii) some methods of deriving the velocity fields, (e.g., adopting the intensity-weighted mean velocity of a profile) can lead to an underestimate of the derived rotation curve (e.g., Bosma 1978; Paper I; de Blok et al. 2008). In addition, in some cases derived rotation curves may have been affected by noncircular motions (e.g., Rhee et al. 2004; Spekkens & Sellwood 2007; Valenzuela et al. 2007).

Given that beam smearing has been ignored in many of the previous studies, that some of the galaxies in those studies have high inclinations, and that the majority of those studies used intensity-weighted mean velocity fields, it is likely that the inner slopes of the rotation curves in those previous studies

have been underestimated. Because such an underestimate of the inner slope limits how much the contribution of the stellar disk can be scaled in a maximum disk fit, an underestimate of the inner slope directly results in an underestimate of ξ .

It is beyond the scope of this paper to review each rotation curve in the literature in detail and assess whether systematic effects may have played a role. However, it is useful to consider as an example the well-studied prototype dwarf galaxy DDO 154. From H I synthesis observations of this galaxy a slowly rising rotation curve was derived, and mass modeling indicated that DDO 154 was almost entirely dominated by dark matter (Carignan & Freeman 1988; Carignan & Beaulieu 1989). Based on the published mass model, we estimate that $\xi = 0.52$, much lower than the values found for our sample. Those early observations had a resolution of $45''$, and the derivation of the rotation curve was certainly affected by beam smearing, especially given the galaxy's inclination of approximately 66° (de Blok et al. 2008).

Recently, de Blok et al. (2008) presented higher resolution H I data for this galaxy. Because of the $12''$ resolution, and the fact that the velocity field was derived using skewed Gaussians, which can account for asymmetries often observed in line profiles, the derived rotation curve is less prone to the systematic effects discussed here. The rotation curve derived by de Blok et al. (2008) rises somewhat more steeply than the one derived earlier by Carignan & Beaulieu (1989), and de Blok et al. (2008) find $\xi = 0.62$. However, the position-velocity diagram shown in Figure 81 of de Blok et al. (2008) suggests that the rotation curve in the inner $2'$ could be even steeper. Indeed, a new study of the kinematics of DDO 154 in the central regions based on long-slit spectroscopy and integral-field spectroscopy (Swaters et al., in preparation) shows a rotation curve that rises somewhat more steeply than the one of de Blok et al. (2008), resulting in a value of $\xi = 0.80$.

A key feature of the sample presented in this paper is that the systematic effects mentioned above were avoided as much as possible. The sample galaxies have inclinations between 39° and 80° and galaxies with large asymmetries were excluded. The rotation curves were derived with an interactive technique using modeling of the observed data cube to correct for the effects of beam smearing (Paper III).

5.3. Mass to light ratios of the stellar disk

For the maximum disk models, the derived mass to light ratio Υ_*^R is tightly coupled to surface brightness, with lower surface brightness galaxies having higher Υ_*^R . This is expected in order to explain the high mass density needed for the maximum disk despite the LSB nature of the stellar disks. The values for Υ_*^R required in the maximum disk models, reach as high as $\Upsilon_*^R = 15$, well outside the range of what population synthesis models predict (e.g., Bell et al. 2003; Zibetti et al. 2009). The precise value of Υ_*^R as derived from such population synthesis may be uncertain by a factor of 2 to 4 (Portinari et al. 2004), and possibly even higher (Bershady et al. 2010). However, even considering these uncertainties, values as high as $\Upsilon_*^R = 15$ appear unlikely, as they would require a strong bias in the initial mass function towards low-mass stars, or a large fraction of the stellar mass being locked up in stellar remnants.

The presence of a nonstellar component of mass with a distribution similar to that of the stars, e.g., in the form of cold molecular gas as suggested by Pfenniger & Combes (1994) and Revaz et al. (2009), could provide an explanation.

Alternatively, the stellar disks may be somewhat less than maximal. Independent measurements of Υ_* from stellar velocity dispersions in spiral galaxies suggest that stellar disks have a submaximum contribution to the rotation curve, with a peak contribution of the stellar disk to the rotation curve of around 65% (Bottema 1993; Westfall et al., in preparation). At this level, the stellar disk still determines the inner shape of the rotation curve, i.e., one would still expect to find $\xi \sim 1$. If the stellar disks would also contribute around 65% in late-type dwarf galaxies, this would reduce Υ_*^R by almost a factor of 2.5. This would bring the mean and maximum Υ_*^R of the galaxies in our sample to 3 and 6, respectively, still above what population synthesis models predict.

If Υ_*^R is assumed to be near unity, as predicted by stellar population synthesis models (see Section 3.4), then well-fitting mass models are found as well. In this case, all galaxies except UGC 7577 are dominated by dark matter. Moreover, the relative contribution of dark matter increases towards lower surface brightness, and the contribution of the disk decreases correspondingly. Thus, for models with $\Upsilon_* \sim 1$, we reach the same conclusions as are usually found for dwarf and LSB galaxies (e.g., Carignan & Beaulieu 1989; Broeils 1992a; de Blok & McGaugh 1997).

There is, however, a critical difference. In many of those previous studies, as described above, low values for ξ were derived. For our sample, however, we find a value for ξ that is near unity. This not only means that the stellar disk can be scaled to explain most of the inner parts of the observed rotation curve. If $\Upsilon_*^R \sim 1$, this also means that the rotation curve of the stellar disk alone must have the same shape as that of the dark matter that dominates the potential. Otherwise, ξ could not be near unity.

In spite of the uncertainties in Υ_*^R , one result from this analysis is firm: the fact that the contribution of the stellar disk can be scaled up to explain the inner parts of the rotation curve indicates that the shapes of the rotation curve of the stellar disk and of the observed rotation curve are similar. There appears to be a strong coupling between the distribution of the stars

and that of the total mass (see also Sancisi 2004; Paper III).

6. CONCLUSIONS

We have presented mass models for a sample of 18 late-type dwarf galaxies. For this sample, the systematic effects due to beam smearing, intensity-weighted-mean velocity fields, high inclination, and noncircular motions were avoided as much as possible. We have analyzed the rotation curves of the galaxies in our sample by fitting mass models consisting of a stellar disk, a gaseous disk and the contribution of an isothermal halo, and we have reached the following conclusions:

- (1) Dwarf galaxies are not necessarily dominated by dark matter within their optical radii. The rotation curve of the stellar disk can be scaled up to explain most of the inner parts of the observed rotation curves. The maximum disk mass models are similar to those for spiral galaxies, with similar fraction of dark matter within a radius of four disk scale lengths. However, the required stellar mass-to-light ratios are high, up to about 15 in the R -band.
- (2) For the maximum disk models, the contribution of the stellar disk to the rotation curve is about 90% at two disk scale lengths, independent of surface brightness or luminosity. The maximum-disk Υ_* is correlated with surface brightness.
- (3) Well fitting mass models can be obtained by assuming that the contribution of the stellar disk to the rotation is maximal, but also by assuming it is negligible. This demonstrates that mass models for late-type dwarf galaxies suffer from the same indeterminacies as those for spiral galaxies.
- (4) If the stellar mass-to-light ratios are set to the values predicted by stellar population synthesis modeling, the relative contribution of the stellar disk decreases with surface brightness, while the relative fraction of dark matter increases.
- (5) Whatever the contribution of the stellar disk to the rotation curve, the similarity in shapes between the rotation curve expected for the stellar disk and the observed rotation curve implies that in the inner parts of late-type dwarf galaxies the total mass density distribution is closely coupled to the luminous mass density distribution.

REFERENCES

- Begeman, K., 1987, PhD thesis, Rijksuniversiteit Groningen (<http://irs.ub.rug.nl/ppn/291578543>)
- Bekki, K., & Stanimirović, S. 2009, MNRAS, 395, 342
- Bell, E.F. & de Jong, R.S. 2001, ApJ 550, 212
- Bell, E.F. Baugh, C.M., Cole, S., Frenk, C.S. & Lacey, C.G. 2003, MNRAS 343, 367
- Bershady, M.A., Verheijen, M.A.W., Westfall, K.B., Andersen, D.R., Swaters, R.A. & Martinsson, T., 2010, ApJ 716, 234
- Binggeli, B., Popescu, C.C., 1995, A&A 298, 63
- Bizyaev, D. & Kajsın, S. 2004, ApJ 613, 886
- Boselli, A., Lequeux, J. & Gavazzi, G. 2002 Ap&SS 281 129
- Bosma, A., 1978, PhD thesis, Rijksuniversiteit Groningen
- Bosma, A. 1981, AJ, 86, 1825
- Bottema, R., 1993, A&A 275, 16
- Bottema, R., Shostak, G.S., van der Kruit, P.C., 1986, A&A 167, 34
- Broeils, A.H., 1992a, PhD thesis, Rijksuniversiteit Groningen
- Broeils, A.H., 1992b, A&A 256, 19
- Buyle, P., Michielsen, D., de Rijcke, S., Ott, J. & Dejonghe, H. 2006, MNRAS 373, 793
- Carignan, C., 1985, ApJ 299, 59
- Carignan, C., Beaulieu, S., 1989, ApJ 347, 760
- Carignan, C., Freeman, K.C., 1988, ApJ 332, 33
- Carignan, C., Sancisi, R., van Albada, T.S., 1988, AJ 95, 37
- Casertano, S., 1983, MNRAS 203, 735
- Casertano, S., & van Gorkom, J. H. 1991, AJ, 101, 1231
- Côté, S., 1995, PhD thesis, Australian National University
- Côté, S., Carignan, C., Sancisi, R., 1991, AJ 102, 904
- Côté, S., Freeman, K.C., Carignan, C., 1997, in Dark and Visible Matter in Galaxies, eds. M. Persic, P. Salucci, A.S.P. conf. ser., vol. 117, p. 52
- Côté, S., Carignan, C., & Freeman, K. C. 2000, AJ, 120, 3027
- de Blok, W. J. G., & McGaugh, S. S. 1997, MNRAS, 290, 533
- de Blok, W.J.G., van der Hulst, J.M. & Bothun, G.D., 1995, MNRAS 274, 235
- de Blok, W.J.G., Walter, F., Brinks, E., Trachternach, C., Oh, S.-H. & Kennicutt, R. C., 2008, AJ 136, 2648
- de Grijs, R., 1997, PhD thesis, Rijksuniversiteit Groningen (<http://irs.ub.rug.nl/ppn/163655375>)
- Dutton, A. A., Courteau, S., de Jong, R., & Carignan, C. 2005, ApJ, 619, 218
- Hoekstra, H., van Albada, T. S., & Sancisi, R. 2001, MNRAS, 323, 453
- Israel, F.P., Tacconi, L.J., Baas, F., 1995, A&A 295, 599
- Jobin, M., Carignan, C., 1990, AJ 100, 648
- Kalnajs, A.J., 1983, in: Internal Kinematics of Galaxies, IAU Symp. 100, ed. E. Athanassoula (Dordrecht: Reidel), p. 87
- Kent, S.M., 1986, AJ 91, 1301
- Kent, S. M. 1987, AJ 93, 816
- Kim, S., Staveley-Smith, L., Dopita, M.A., Freeman, K.C., Sault, R.J., Kesteven, M.J., McConnell, D., 1998, ApJ 503, 674
- Lake, G., Schommer, R.A., van Gorkom, J.H., 1990, AJ 99, 547
- Martimbeau, N., Carignan, C., Roy, J.-R., 1994, AJ 107, 543
- Meurer, G.R., Carignan, C., Beaulieu, S.F., Freeman, K.C., 1996, AJ 111, 1551
- Milgrom, M., 1983, ApJ 270, 365
- Nilson, P. 1973, Uppsala General Catalogue of Galaxies, Uppsala Astr. Obs. Ann., Vol. 6

- Noordermeer, E., 2006, PhD thesis, Rijksuniversiteit Groningen
<http://irs.ub.rug.nl/ppn/292030207>
- Persic, M., Salucci, P., & Stel, F. 1996, MNRAS, 281, 27
- Pfenniger, D., Combes, F., 1994, A&A 285, 94
- Portinari, L., Sommer-Larsen, J., & Tantaló, R. 2004, MNRAS, 347, 691
- Puche, D., Carignan, C. & Bosma A., 1990, AJ 100, 1468
- Puche, D., Carignan, C. & Wainscoat, R.J., 1991, AJ 101, 456
- Revaz, Y., Pfenniger, D., Combes, F., & Bournaud, F. 2009, A&A, 501, 171
- Rhee, G., Valenzuela, O., Klypin, A., Holtzman, J., & Moorthy, B. 2004, ApJ, 617, 1059
- Sackett, P. D. 1997, ApJ, 483, 103
- Sanders, R.H., 1996, ApJ 473, 117
- Sancisi, R., 2004, IAU Symp. 220, ASP Conf series, p. 223
- Sancisi, R. & Allen, R.J. 1997, A&A 74, 73
- Schwarzkopf, U. & Dettmar, R.-J. 2000, A&A361, 451
- Sicotte, V., Carignan, C., 1997, AJ 113, 609
- Simon, J.D., Bolatto, A.D., Leroy, A. & Blitz L., 2003, ApJ 596, 957
- Skillman, E.D., Bothun, G.D., Murray, M.A., Warmels, R.H., 1987, A&A185, 61
- Spekkens, K., & Sellwood, J. A. 2007, ApJ, 664, 204
- Steigman, G., 2007, Annual Review of Nuclear and Particle Science, 57, 463
- Sung et al., 1998, ApJ 505, 199
- Swaters, R.A., 1999, PhD thesis, Rijksuniversiteit Groningen (S99,
<http://irs.ub.rug.nl/ppn/186373880>)
- Swaters, R. A., & Balcells, M. 2002, A&A, 390, 863 (Paper II)
- Swaters, R. A., Madore, B. F., & Trewhella, M. 2000, ApJ, 531, L107
- Swaters, R.A., van Albada, T. S., van der Hulst, J. M. & Sancisi, R. 2002 A&A 390, 829 (Paper I)
- Swaters, R. A., Madore, B. F., van den Bosch, F. C., & Balcells, M. 2003, ApJ, 583, 732
- Swaters, R.A., Sancisi, R., van Albada, T. S. & van der Hulst, J. M. 2009 A&A 493, 871 (Paper III)
- Valenzuela, O., Rhee, G., Klypin, A., Governato, F., Stinson, G., Quinn, T., & Wadsley, J. 2007, ApJ, 657, 773
- van Albada, T.S., Bahcall, J.N., Begeman, K., Sancisi, R., 1985, ApJ 295, 305
- van Albada, T.S., Sancisi, R., 1986, Phil. Trans. R. Soc. Lond. A 320, 447
- van den Bergh, S., 1988, PASP 100, 344
- van den Bosch, F.C. & Swaters, R.A. 2001, MNRAS 325, 1017
- van Zee, L., Haynes, M.P., Salzer, J.J., Broeils, A.H., 1997, AJ 113, 1618
- Verheijen, M.A.W., 1997, PhD thesis, Rijksuniversiteit Groningen
(<http://irs.ub.rug.nl/ppn/163958270>)
- Verheijen, M. A. W., & Sancisi, R. 2001, A&A, 370, 765
- Weldrake, D.T.F., de Blok, W.J.G. & Walter F., 2003, MNRAS 340, 12
- Zibetti, S., Charlot, S. & Rix, H.-W. 2009, MNRAS 400, 1181